Pergamon

Int. J. Heat Mass Transfer. Vol. 40, No. 2, pp. 365–377, 1997

0017–9310/97 $15.00 + 0.00

PII: S0017–9310(96)00097–X

The isolated bubble regime in pool nucleate boiling

Yu. A. BUYEVICH and B. W. WEBBON
NASA Ames Research Center, Moffett Field, CA 94035, U.S.A.

(*Received* 14 *August* 1995 *and in final form* 6 *March* 1996)

Abstract—We consider an isolated bubble boiling regime in which vapour bubbles are intermittently produced at a prearranged set of nucleation sites on an upward facing overheated wall plane. In this boiling regime, the bubbles depart from the wall and move as separate entities. Heat transfer properties specific to this regime cannot be described without bubble detachment size, and we apply our previously developed dynamic theory of vapour bubble growth and detachment to determine this size. Bubble growth is presumed to be thermally controlled. Two limiting cases of bubble evolution are considered: the one in which buoyancy prevails in promoting bubble detachment and the one in which surface tension prevails. We prove termination of the isolated regime of pool nucleate boiling to result from one of the four possible causes, depending on relevant parameters values. The first cause consists in the fact that the upward flow of rising bubbles hampers the downward liquid flow, and under certain conditions, prevents the liquid from coming to the wall in an amount that would be sufficient to compensate for vapour removal from the wall. The second cause is due to the lateral coalescence of growing bubbles that are attached to their corresponding nucleation sites, with ensuing generation of larger bubbles and extended vapour patches near the wall. The other two causes involve longitudinal coalescence either: (1) immediately in the wall vicinity, accompanied by the establishment of the multiple bubble boiling regime or (2) in the bulk, with the formation of vapour columns. The longitudinal coalescence in the bulk is shown to be the most important cause. The critical wall temperature and the heat flux density associated with isolated bubble regime termination are found to be functions of the physical and operating parameters and are discussed in detail.

1. INTRODUCTION

It is fairly well known that, as wall temperature passes over a critical threshold value, it becomes impossible to maintain the initial boiling regime that is characterized by the generation of a lot of single vapour bubbles on a superheated wall, so that these bubbles thereafter preserve their individuality. As wall temperature grows, the isolated bubble regime of nucleate boiling is first replaced by a transient boiling regime in which the wall intermittently borders on occasional liquid and vapour patterns. At still larger wall temperatures, the isolated bubble regime is replaced by a film boiling regime in which the wall is separated from the liquid by a stable vapour film, and liquid evaporation and irregular vapour slug formation occur at the free film surface. Termination of the isolated bubble regime presents a certain crisis of pool nucleate boiling. This crisis does not necessarily coincide with the usually studied boiling crisis in which maximal critical heat flux (CHF) is attained. Nevertheless, the heat flux densities associated with both these crises are understandably of primary concern in the design, operation, and safety of various boiling and two-phase flow devices. For this reason, there are a great many experimental and theoretical studies exclusively aimed to provide a better insight into the underlying physics of the mechanisms of both pool nucleate and forced convection boiling, and to understand the key factors that may be responsible for the observed alteration of these mechanisms (for example, see a review in ref. [1]).

The isolated bubble boiling regime was studied in a great many papers. From a phenomenological point of view, we also know what follows termination of this regime. According to Zuber [2], as wall temperature grows, the spacing decreases between a bubble developing at a nucleation site and its predecessor departed from the same site, and as wall temperature exceeds some critical level, these two bubbles merge to form a new mushroom-like bubble This merging process can also involve other bubbles originated at this site, and formation of tandems consisting of large bubbles followed by much smaller bubbles sometimes occurs. The resultant boiling regime is characterized by non-uniformly sized bubbles and is sometimes referred to as a "multiple bubble" regime.

Alternatively, as wall temperature increases, longitudinal bubble coalescence becomes possible in the bulk above the wall, and this process results in the generation of swirling vapour jets, or columns, attached to the wall at nucleation sites. The vapour columns are either shattered into small bubbles, or they lose their hydrodynamic stability and merge, thus giving rise to vapour patches or blankets covering a considerable area of the wall. These hovering patches

NOMENCLATURE

C growth constant, equation (6)
c_l liquid specific heat capacity
D bubble diameter
f bubble detachment frequency
g gravity acceleration
K_u bubble detachment frequency, equation (21)
L specific latent heat of evaporation
L_s, L_t length and time scales, equation (4)
l average distance between neighbouring nucleation sites
N_J Jakob number, equation (6)
N_n nucleation site population density number, equation (32)
N_σ surface tension number, equation (5)
n nucleation site concentration
Q_l, Q_v volume fluxes of liquid and vapour
q heat flux density
R bubble radius
s distance separating bubble centre from the wall
T temperature
ΔT $T_w - T_s$
t time
U_b, U_b^∞ rise bubble velocity for bubble swarm and for a single bubble in an unbounded liquid
W_l, W_v averaged liquid and vapour velocities in the bulk
x variable defined in equations (44) and (47).

Greek symbols
χ liquid thermal diffusivity
ϕ bubble volume concentration in the bulk
ϕ_m maximal bubble volume concentration
κ density ratio, ρ_v/ρ_l
ξ, ζ dimensionless bubble radius and bubble centre coordinate
ρ density
σ surface tension coefficient
τ dimensionless time.

Subscripts
d detachment
e normal (Earth) conditions
l liquid
s saturation
v vapour
w wall
∞ far from the wall
I, II, III and IV pertain to critical quantities.

are linked to the wall by a number of vapour stems and continue to grow since they are being fed by vapour through these stems. The same patches can also appear due to the lateral coalescence of bubbles evolving at neighbouring nucleation sites. Sufficiently extended patches can be justifiably regarded as initial fluctuating vapour film patterns, and irregular vapour slugs are generated at their external boundaries.

Although the above description is basically correct, and the patterns described have been repeatedly observed in many works, the exact conditions that give rise to these patterns during breakup of the isolated bubble regime remain unknown to date. To discover these conditions, we first need a reliable model of the isolated bubble regime of pool nucleate boiling, and this implies, in turn, that bubble detachment characteristics must be determined as functions of all relevant parameters. When treating both isolated bubble regime properties and the conditions for regime termination, we intend to use our newly developed bubble growth and detachment theory [3, 4].

Many empirical and semi-empirical formulae exist that describe heat flux, bubble formation frequency, etc., in the isolated bubble regime of pool nucleate boiling. Since the most important of these formulae will be reproduced on a relatively stringent basis later, there is no need to write them down and discuss them in this section.

Although the CHF crisis does not necessarily coincide with the isolated bubble regime collapse (and so is not of primary concern in this paper), we briefly mention available models proposed to describe the CHF crisis (these models are reviewed at some length in refs. [1, 5, 6]). These models can seemingly be classified into three main groups.

The first group comprises models in which it is suggested that bubbles attached to nucleation sites reach critical packing and then merge as the total number of the sites increases with the heated surface superheat, and as a final result, the bubbles blanket the wall with vapour [7]. This blanketing presumably interrupts an incessant fresh liquid flow to the wall, thereby causing the surface to dry out. Those models are limited in the respect that, while taking into account the dependence on temperature of active nucleation site population density, they often fail to allow for a similar dependence of bubble departure diameter on temperature, as detected in [8].

Models of the second group are based on concepts relating to Taylor and Helmholtz hydrodynamic stability of (1) vapour films adjacent to the wall and (2) vapour columns originated as bubbles rising in suc-

cession overtake one another and coalesce in the longitudinal direction. The onset of instability is assumed to set a limit to the vapour removal process accomplished by departed bubbles, and hence to result in heated surface dryout as well [9–12].

Models of the third group usually postulate that, on the verge of reaching CHF, vapour is removed from the wall through narrow stems that are anchored to nucleation sites and that feed a vapour mass above the stems [6, 13]. This vapour mass entraps a liquid macrolayer vaporization of which ensures heat removal from the wall. The CHF is assumed to occur when macrolayer lifetime becomes smaller than the characteristic lifetime of the vapour mass hovering above the wall. If this condition is satisfied, the macrolayer has time enough to completely evaporate before the vapour mass departs from the wall, thus leading to dryout. This model received much attention in recent years and formed a foundation for numerous studies of high-heat-flux boiling (e.g. [14, 15]).

Very substantial difficulties additionally arise when attempting to model the CHF crisis under the more complicated conditions of forced convection boiling [6], not to mention those of boiling of subcooled liquids [16, 17] and of boiling with time-dependent heat input [18, 19]. However, our objective in the present paper is to address the crisis that makes the isolated bubble boiling regime come to an end, but by no means the crisis that brings about CHF.

In order to simplify the subsequent analysis and to get a comparatively transparent physical picture of the effects caused by macroscopic bubble properties, we presume that (1) the heated surface is an extended, upward facing flat wall and (2) the wall material thermal diffusivity is much larger than that for the liquid above the wall, so that wall temperature fluctuations due to cyclical formation of bubbles at nucleation sites can be ignored. We also assume that bubble growth is thermally controlled which gives an opportunity to directly use the results obtained in refs. [3, 4].

2. PROPERTIES OF THE ISOLATED BUBBLE REGIME

In this section, we address the isolated bubble regime of pool boiling, meaning that vapour bubbles grow at their nucleation sites, detach themselves from these sites, and then rise above the wall as separate entities, that is, without coalescence. Conditions under which this regime can be maintained will be revealed later on. In steady-state boiling, upward vapour flow produced by rising bubbles must be exactly compensated by downward liquid flow to the wall, that is, the material balance equation must hold true,

$$\rho_v Q_v = \rho_l Q_l. \tag{1}$$

Assuming that the artificial nucleation sites under consideration produce vapour bubbles with no appreciable waiting time, vapour volume flux can be expressed as follows:

$$Q_v = \frac{4}{3}\pi R_d^3 f n = \frac{4}{3}\pi \frac{R_d^3}{t_d} n \tag{2}$$

nucleation site number concentration n being a function of wall temperature, and this function also depends on the surface properties of the wall, as well as on its affinity to the liquid. In a particular case of walls with artificial nucleation cavities, n may be regarded as a known constant [20].

The total heat flux from the wall has to be formulated in the form

$$q = \rho_l[c_l(T_s - T_\infty) + L]Q_l = \rho_v[c_l(T_s - T_\infty) + L]Q_v. \tag{3}$$

This equation is rigorous for boiling heat removal from an infinite upward facing plate, and without forced convection, irrespective of the peculiarities of convective heat transfer in the liquid near the wall. This equation can be formally derived by considering energy balance in the system. According to equation (3), the heat flux is composed of two constituents: one due to heating the liquid that is incessantly coming to the wall from the bulk up to the saturation temperature, and the other due to the absorption and transfer of latent heat of evaporation by rising bubbles. Equation (3) is valid for an arbitrary wall superheat, the heat flux depending on wall superheat in an implicit way, through Q_v (or Q_l).

To make equation (3) fully determinate, we need representations for bubble detachment radius R_d and for total time t_d of bubble growth till detachment. These quantities can be found with the help of the theory in refs. [3, 4]. Neglecting evaporation from the liquid macrolayer separating a vapour bubble from the wall as compared with evaporation from the bulk of the ambient liquid (what is permissible to do for liquids whose Prandtl number is not exceedingly small), also introducing time and length scales as well as corresponding dimensionless variables as

$$R = L_s\xi \quad s = L_s\zeta \quad t = L_t\tau$$

$$L_t \approx 0.779\left(\frac{1+1.455\kappa}{1-\kappa}\right)^{2/3}\frac{(CN_J)^{2/3}\chi^{1/3}}{g^{2/3}} \quad \kappa = \frac{\rho_v}{\rho_l},$$

$$L_s \approx 0.883\left(\frac{1+1.455\kappa}{1-\kappa}\right)^{1/3}\frac{(CN_J)^{4/3}\chi^{2/3}}{g^{1/3}} \tag{4}$$

we arrive at equations governing dimensionless bubble radius ξ and dimensionless distance ζ that separates the bubble centre from the wall [3, 4]

$$\xi = \sqrt{\tau} \quad \frac{d}{d\tau}\left(\tau^{3/2}\frac{d\zeta}{d\tau}\right) = \tau^{3/2} + N_\sigma\frac{\tau-\zeta^2}{\sqrt{\tau}}$$

$$N_\sigma \approx \frac{0.963}{1+1.455\kappa}\frac{\sigma/\rho_l}{(CN_J)^{8/3}\chi^{4/3}g^{1/3}}. \tag{5}$$

In equations (4) and (5), N_J is the Jakob number and constant C is of the order of unity and characterizes bubble growth rate in conformity with the Fritz's formula,

$$N_J = \frac{(\lambda/\chi)\,\Delta T}{\rho_v L} \quad \Delta T = T_w - T_s \quad \frac{dR}{dt} = \frac{CN_J}{2}\left(\frac{\chi}{t}\right)^{1/2}. \tag{6}$$

In refs. [3, 4] two forces are shown to ensure bubble detachment: (1) buoyancy and (2) a force due to surface tension effects. The relative role played by the surface tension force as compared with buoyancy is characterized by parameter N_σ. It is worth noting that equations (4) and (5) do not involve any adjustable parameters save for growth constant C.

Initial conditions for ζ may be imposed with the help of asymptotical solution $\zeta \approx 2N_\sigma\tau/3$ which is approximately valid at $\tau \ll N_\sigma$. When ζ becomes equal to ξ, evolution of a vapour bubble attached to a nucleation site terminates, and the bubble departs from the wall. Dimensionless bubble evolution time must be found by numerically integrating equation (5) under the initial conditions specified above. This evolution time is a decreasing function of N_σ, and $\tau_d \approx 2.924$ if N_σ is small enough, that is, if buoyancy dominates the surface tension force in aiding bubble detachment [3, 4]. The dimensionless bubble evolution time is plotted in Fig. 1 as a function of N_σ. We can easily prove that τ_d can be approximated, with a sufficiently high accuracy, by equations

$$\tau_d \approx \text{const} \approx 2.9 \quad \text{at } N_\sigma \leqslant 0.1$$

$$\tau_d \approx 1.53 N_\sigma^{-5/8} \quad \text{at } N_\sigma \geqslant 1. \tag{7}$$

The first equation (7) corresponds to situations where buoyancy is practically the only force that provides for bubble detachment. The second equation (7) bears upon situations in which bubble detachment is mostly due to the surface tension force, except for the very final detachment stage where buoyancy is relevant no matter how low gravity acceleration may be. As N_σ increases, departing bubbles become smaller and their detachment frequency grows [3, 4].

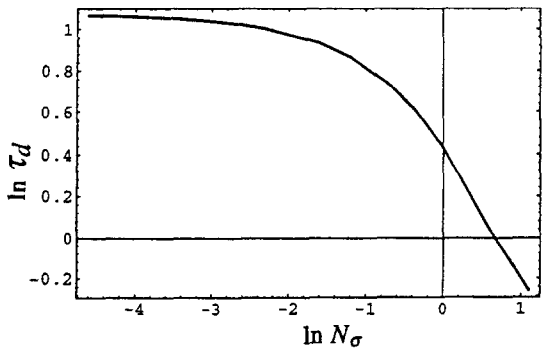

Fig. 1. Dimensionless bubble detachment time as a function of parameter N_σ.

Dimensional bubble evolution time and bubble detachment radius must be expressed through τ_d in accordance with equation (4). At small N_σ (that is, under conditions of bubble detachment from the wall being due to buoyancy) we get

$$t_d = L_t\tau_d \approx 2.26\left(\frac{1+1.455\kappa}{1-\kappa}\right)^{2/3}\frac{(CN_J)^{2/3}\chi^{1/3}}{g^{2/3}}$$

$$R_d = L_s\sqrt{\tau_d} \approx 1.50\left(\frac{1+1.455\kappa}{1-\kappa}\right)^{1/3}\frac{(CN_J)^{4/3}\chi^{2/3}}{g^{1/3}}. \tag{8}$$

In the literature, equations relating bubble departure diameter and bubble detachment frequency are very popular. It is easy to derive such equations from equation (8). If one chooses to exclude thermophysical parameters, one gets ($f \equiv 1/\tau_d$)

$$f\sqrt{D_d} \approx 0.77\left(\frac{1-\kappa}{1+1.455\kappa}\right)^{1/2}\sqrt{g}. \tag{9}$$

Alternatively, if one prefers to exclude gravity acceleration, one arrives at

$$D_d\sqrt{f} \approx 2.0(CN_J)\sqrt{\chi}. \tag{10}$$

Equations of the same type as equations (9) and (10) were proposed over and over again on empirical or semi-empirical grounds. In particular, equations that differ from equation (9) at $\kappa \ll 1$ only by numerical coefficients were earlier put forward in a number of works according to which the coefficient of 0.77 in equation (9) should be substituted by 1.15 [21], 0.56 [22] or 0.90 [23]. An equation of the form (10) was recently suggested in ref. [24], with a coefficient of $3\pi^{1/2}/4 \approx 1.33$ instead of $2C$ involved in equation (10).

At large N_σ (that is, under conditions in which the surface tension force prevails in bubble detachment from the wall), the second equation (7) holds true, and we obtain other equations, instead of equations (8),

$$t_d \approx 1.220\frac{(1+1.455\kappa)^{31/24}}{(1-\kappa)^{2/3}}\frac{(CN_J)^{7/3}\chi^{7/6}}{g^{11/24}(\sigma/\rho_l)^{5/8}}$$

$$R_d \approx 1.105\frac{(1+1.455\kappa)^{31/48}}{(1-\kappa)^{1/3}}\frac{(CN_J)^{13/6}\chi^{13/12}}{g^{11/48}(\sigma/\rho_l)^{5/16}}. \tag{11}$$

In this case, equations (9) and (10) are replaced by

$$fD_d^{14/13} \approx 1.925\frac{(1-\kappa)^{4/13}}{(1+1.455\kappa)^{31/52}}g^{11/52}\left(\frac{\sigma}{\rho_l}\right)^{15/52} \tag{12}$$

$$D_d\sqrt{f} \approx 2.00(CN_J)\sqrt{\chi}. \tag{13}$$

Interestingly, equation (13) coincides with previously derived equation (10). Thus, the product that appears in the left-hand side of these equations is independent of N_σ, and this mere fact makes this product especially usable when correlating experimental data. Equation (12) resembles empirical power laws

expressing fD_d in terms of g and σ/ρ_l (e.g., refs. [2, 23]), but the exponents involved have slightly different values. However, this difference is likely to fall within experimental error limits, and these are usually rather broad.

Heat flux can be formulated from equations (2)–(4) in the following way:

$$q = \frac{4}{3}\pi\rho_v[c_l(T_s - T_\infty) + L]n\frac{L_*^3}{L_t}\sqrt{\tau_d(N_\sigma)}. \quad (14)$$

Using equation (7), this gives at $N_\sigma \leqslant 0.1$

$$q \approx 6.30\left(\frac{1+1.455\kappa}{1-\kappa}\right)^{1/3} \times \frac{(CN_J)^{10/3}\chi^{5/3}}{g^{1/3}} n\rho_v[c_l(T_s - T_\infty) + L] \quad (15)$$

and at $N_\sigma \geqslant 1$

$$q \approx 4.58\frac{(1+1.455\kappa)^{31/48}}{(1-\kappa)^{1/3}} \times \frac{(CN_J)^{25/6}\chi^{25/12}}{g^{11/48}(\sigma/\rho_l)^{5/16}} n\rho_v[c_l(T_s - T_\infty) + L]. \quad (16)$$

Equations (14)–(16) completely describe heat transfer due to the isolated bubble boiling regime. They are applicable to both saturated and subcooled boiling. In particular, these equations show how heat flux dependence on both physical and operating parameters is intensified by enhancing the role played by the surface tension force in detaching bubbles from their nucleation sites. As N_σ increases, heat flux dependence on wall overheat $T_w - T_s$ progressively becomes steeper (if n is constant, the relevant exponent monotonously grows from 10/3 to 25/6), and its dependence on thermophysical parameters correspondingly becomes stronger. However, heat flux dependence on liquid subcooling does not change, whereas its dependence on gravity considerably weakens. What is especially important is that heat flux becomes dependent on surface tension at the liquid–vapour interface as N_σ increases, even if n is constant. This dependence is brought about by the fact that bubble detachment characteristics become dependent on the surface tension coefficient in a region of appreciable N_σ, and it has nothing to do with the anticipated influence of surface tension on nucleation site activation and on formation of initial vapour nuclei. For real surfaces with no artificial nucleation cavities that are commonly encountered in practice, this simple picture is obliterated by the mere fact that nucleation site concentration n is also dependent on both wall overheat and surface tension coefficient.

The dependence of heat flux on pressure in the isolated bubble boiling regime is represented by equations (15) and (16) in an implicit form: through vapour density ρ_v and density ratio κ. Heat transfer is substantially augmented as pressure grows, and especially so as the vapour density approaches the density of the liquid. When comparing equations (15) and (16), it is not difficult to see that an increase in N_σ results in a slight enhancement of the heat flux dependence on pressure.

It is worth stressing once again that the above formulae do not involve arbitrary adjustable parameters and empirical coefficients except for growth rate constant C that is involved in almost all the above formulae due to its appearance in the definition both of time and length scales and of dimensionless criteria. This constant varies from 1.13 to 2 depending on the model chosen to describe heat transfer to a bubble growing within a superheated liquid layer near the wall. However, when raised to a high power, this variation brings about an uncertainty in numerical coefficients involved in the heat flux equations which can amount to an order of magnitude. Hence it becomes evident that, in order to obtain reliable values for those coefficients, the bubble evolution theory must be made more precise even in the case where bubble growth is assumed to be thermally controlled and where the bubbles are viewed as submerged into a superheated liquid layer near the wall.

However, this uncertainty in C does not affect in any way the dependence of the resultant formulae on the dimensional physical and operating parameters, and these formulae are independent of other adjustable coefficients. This very fact should be regarded as a substantial advantage of our model as compared with numerous conventional models.

3. TWO-PHASE FLOW CRISIS IN THE BULK

Let us consider, next, vapour removal from the wall that is effected by rising bubbles. Within a region high above the wall where upward bubble motion and downward liquid flow are stabilized, the vapour and liquid volume fluxes are expressible as

$$Q_v = \phi(U_b - W_l) = \phi W_v \quad Q_l = (1-\phi)W_l \quad (17)$$

vapour and liquid velocities being directed upward and downward, respectively. Combining this with material balance equation (1), we obtain

$$W_v = \frac{1-\phi}{1-(1-\kappa)\phi}U_b \quad W_l = \frac{\kappa\phi}{1-(1-\kappa)\phi}U_b \quad (18)$$

and allowing for equation (3), we further derive

$$\frac{\phi(1-\phi)}{1-(1-\kappa)\phi}U_b = \frac{q}{\rho_l[c_v(T_s - T_w) + L]}. \quad (19)$$

Bubble velocity U_b depends on bubble volume fraction ϕ. Both experimental [25] and theoretical [26] studies yield the well-known formula:

$$U_b = (1-\phi)U_b^\circ \quad (20)$$

with U_b° standing for the rise velocity of a single bubble

in an unbounded liquid. Single bubble velocity is a complicated function of the bubble Reynolds number. For the sake of definitiveness, in what follows we use the simplest relationship for spheroidal bubbles in the Reynolds number range where bubble velocity is independent of bubble size, namely,

$$U_b^\infty = K_u\left[\frac{\sigma g(\rho_l-\rho_v)}{\rho_l^2}\right]^{1/4} = K_u\left[(1-\kappa)g\frac{\sigma}{\rho_l}\right]^{1/4} \tag{21}$$

where the numerical coefficient ranges from 1.18 [27] to 1.53 [28].

The quantity on the left-hand side of equation (19) cannot exceed its maximal value which it reaches at some $\phi = \phi_m$. If κ is small compared with unity, $\phi_m \approx (1-\kappa)/2$, and the maximal value of the said quantity can be presented, with the same accuracy, as

$$\frac{\phi_m(1-\phi_m)^2}{1-(1-\kappa)\phi_m}U_b^\infty \approx \frac{1-\kappa}{4}U_b^\infty = \frac{K_u}{4}(1-\kappa)^{5/4}\left(g\frac{\sigma}{\rho_l}\right)^{1/4} \tag{22}$$

where equation (21) is taken into account as well. If ϕ exceeds ϕ_m, upward vapour flow cannot be compensated for by downward liquid flow in conformity with the material balance requirement expressed by equation (1). As a result, the steady motion of the bubbles and liquid under consideration becomes impossible, and extended vapour masses will inevitably appear in the vicinity of the wall. This alteration in flow character is of a purely hydrodynamic origin and has much in common with the flooding-up crisis of countercurrent two-phase flows that is often encountered in some apparatuses and devices of chemical and power engineering.

According to equation (19), quantity (22) also determines the maximal heat flux density that can be attained in the isolated bubble boiling regime, if this regime actually breaks up due to flooding-up in the bulk above the wall. No matter how high parameter N_σ may be, this heat flux density can be formulated from equations (19) and (22) in a universal form,

$$q_l \approx \frac{K_u}{4}(1-\kappa)^{5/4}\left(g\frac{\sigma}{\rho_l}\right)^{1/4}\rho_v[c_l(T_s-T_\infty)+L]. \tag{23}$$

It is not at all surprising that this critical flux does not depend on the Jakob number (and consequently, on wall overheat) because (1) critical heat transfer is fully determined by the maximal value of vaporized liquid mass in accordance with equation (3) for both saturated and subcooled boiling and (2) this maximal liquid mass is determined only by the hydrodynamics of the countercurrent two-phase flow above the wall, but not in the least by thermal processes near the wall. As a function of pressure, flux (23) has a maximum in the region of relatively high pressures.

This notwithstanding, the "critical wall overheat" does depend on liquid and vapour thermophysical properties (this overheat corresponds to the isolated bubble regime termination and is not identical to the overheat that is associated with the CHF). This is also quite understandable because wall temperature must be high enough to provide for the emergence of the maximal vapour volume determined in equation (22). This critical overheat can be found by equating flux (23) to the flux expressed on the right-hand side of equation (14). After a simple manipulation, using equation (15) we arrive at the "critical overheat equation"

$$(CN_J)_l \approx 0.40\frac{(1-\kappa)^{19/40}}{(1+1.455\kappa)^{1/10}}\frac{g^{7/40}}{\chi^{1/2}n^{3/10}}\left(\frac{\sigma}{\rho_l}\right)^{3/40} \qquad N_\sigma \leqslant 0.1 \tag{24}$$

and using equation (16) we obtain

$$(CN_J)_l \approx 0.52\frac{(1-\kappa)^{19/50}}{(1+1.455\kappa)^{31/200}} \times \frac{g^{23/200}}{\chi^{1/2}n^{6/25}}\left(\frac{\sigma}{\rho_l}\right)^{27/200} \qquad N_\sigma \geqslant 1 \tag{25}$$

coefficient K_u having been taken equal to 1.18 [27]. Critical wall overheat does not depend on whether the liquid is saturated or not. It should be kept in mind that not only N_J but also n generally depend on wall overheat.

It is worth emphasizing once again that formulae (24) and (25) refer to the simplest case where bubble velocity as expressed by equation (21) is independent of bubble size. Even then, a poorly determinable numerical coefficient K_u is introduced into the theory in addition to C.

The isolated bubble boiling regime actually establishes when wall temperature is low enough to render CN_J smaller than its critical value as defined in accordance with equation (24) or (25), if there is nothing to prevent this regime from termination at smaller wall temperatures. In practice, this is not always the case since prior to the critical wall temperature being reached, bubbles evolving at nucleation sites on a heated wall, as well as detached bubbles rising through the ambient liquid, may well start to interfere and to merge with the formation of larger bubbles, extended fluctuating vapour patches hovering above the wall, and vapour columns anchored to the wall.

4. LATERAL BUBBLE COALESCENCE AT THE WALL

In this section, we address the conditions at which lateral coalescence of bubbles growing at neighbouring nucleation sites necessarily occurs. If $l = an^{-1/2}$ is the distance separating neighbouring nucleation sites, lateral bubble coalescence begins when R_d reaches $l/2$. (Coefficient a is of the order of

unity, its exact value depends on the type of two-dimensional (2D) lattice formed by the nucleation sites. If this lattice is not regular, the above formula for l must be regarded as approximate.) Lateral coalescence can certainly be regarded as well-developed when bubble radius $\langle R\rangle$ averaged over the ensemble of growing bubbles becomes equal to or exceeds $l/2$. In any case, the condition for the onset of lateral coalescence in the isolated bubble regime reads

$$R_d = L_s\sqrt{\tau_d} \propto n^{-1/2}. \tag{26}$$

The fact that groups of bubbles containing a few bubbles have merged themselves into larger bubbles, thus establishing a multiple bubble boiling regime, does not imply that heat transfer properties specific to the isolated bubble regime must necessarily be modified to a considerable extent. Spontaneous merging of groups consisting of several bubbles results only in the detached bubbles being no longer identical but instead being distributed over their size. This certainly does not alter the intrinsic physical nature of the isolated bubble regime of pool nucleate boiling. Equations (23)–(25) for critical heat flux density and critical wall temperature remain precisely the same if ensuing bubble enlargement does not affect bubble velocity as defined by equations (20) and (21).

However, such a situation drastically changes when groups of a sufficiently large number of bubbles coalesce to form an extended vapour blanket that could be looked upon as something like a fluctuating vapour film covering the wall. Nothing definite is known as to how large the number of merged bubbles must be in order to form not still another, larger bubble, but a fluctuating film pattern. In these circumstances, it seems appealing and reasonable to make use of standard concepts used in the percolation theory [29]. In accordance with this theory, a qualitative change occurs in a system of merging objects when, as a result of this merging, it becomes possible for an infinite cluster that includes an infinite number of these objects to originate. For 2D systems, the infinite cluster comes about as the critical surface area fraction occupied by the merging objects reaches the critical value of 1/2 [29]. While neglecting the fact that maximal cross-sections of growing bubbles made by planes parallel to the wall are situated at different distances from the wall, we arrive at the following condition that expresses the aforementioned geometrical requirement:

$$\pi\langle R^2\rangle n = \frac{\pi}{2}R_d^2 n = \frac{\pi}{2}L_s^2\tau_d(N_\sigma)n = \frac{1}{2}. \tag{27}$$

We have also assumed that the age of an arbitrarily chosen bubble is uniformly distributed within interval $(0, t_d)$. Hence, the probability of finding this bubble to have current radius R is proportional to $\tau^{1/2}$ with τ being uniformly distributed in $(0, \tau_d)$. It immediately follows from this assumption and from equations (4) and (5) that $\langle R\rangle = 2R_d/3$ and $\langle R^2\rangle = R_d^2/2$.

It is easy to see that conditions (26) and (27) practically coincide, accurate to an arbitrary constant coefficient of the order of unity that ought to appear in equation (26). This means, in particular, that at a very slight further increase in wall temperature, the occasional coalescence of couples of neighbouring bubbles attached to the wall transforms into the formation of extended vapour patches. For definitiveness, we make use of condition (27) in what follows.

At small values of N_σ, and for both cases of $N_\sigma \leqslant 0.1$ and $N_\sigma \geqslant 1$, equations (8), (25) and (11), (26) yield critical wall overheat equations that identify the critical value of CN_J at which the infinite bubble cluster appears. In the first case, we arrive at

$$(CN_J)_{II} \approx \frac{0.480}{n^{3/8}}\left(\frac{1-\kappa}{1+1.455\kappa}\right)^{1/4}\frac{g^{1/4}}{\chi^{1/2}} \quad N_\sigma \leqslant 0.1 \tag{28}$$

and in the second case, we get

$$(CN_J)_{II} \approx \frac{0.733}{n^{3/13}}\frac{(1-\kappa)^{2/13}}{(1+1.455\kappa)^{31/104}} \times \frac{g^{11/104}}{\chi^{1/2}}\left(\frac{\sigma}{\rho_l}\right)^{15/104} \quad N_\sigma \geqslant 1. \tag{29}$$

If the isolated bubble boiling regime is terminated by lateral coalescence, the critical heat flux density associated with this regime termination can be found from equations (15) or (16) in which the Jakob number is understood to be equal to its critical value as determined in equation (28) or (29), respectively. A simple manipulation yields the following formulae for this critical heat flux density:

$$q_{II} \approx 0.546\left(\frac{1-\kappa}{1+1.455\kappa}\right)^{1/2}\frac{g^{1/2}}{n^{1/4}}\rho_v[c_l(T_s - T_\infty) + L] \quad N_\sigma \leqslant 0.1 \tag{30}$$

$$q_{II} \approx 0.274\frac{(1-\kappa)^{22/9}}{(1+1.455\kappa)^{31/52}}g^{11/52}\left(\frac{\sigma}{\rho_l}\right)^{15/52} \times n^{1/26}\rho_v[c_l(T_s - T_\infty) + L] \quad N_\sigma \geqslant 1. \tag{31}$$

When the critical value of CN_J identified in equation (28) or (29) is smaller than the critical value of the same parameter defined by equation (24) or (25), respectively, then the isolated bubble regime breakup should actually be due to the lateral coalescence of bubbles attached to neighbouring nucleation sites on the wall, rather than to the two-phase flow flooding-up crisis in the bulk above the wall.

In order to find out what happens first as wall temperature increases, the two-phase flow flooding-up crisis or well-developed bubble merging on the wall, we must compare the different critical values of CN_J. At small N_σ, we conclude that formation of large vapour patches due to bubble coalescence precedes

the two-phase flow crisis if the following inequality holds true:

$$N_n = \frac{n}{g}\frac{\sigma}{\rho_l} \geqslant N_{n,1},$$

$$N_{n,1}^{3/40} = \frac{1.20}{(1-\kappa)^{9/40}(1+1.455\kappa)^{3/20}} \quad N_\sigma \leqslant 0.1. \tag{32}$$

At larger N_σ, comparison of the critical quantities in equations (25) and (29) yields, instead of inequality (32), the following inequality as a condition under which developed lateral bubble coalescence occurs at a smaller wall temperature instead of two-phase flow crisis occurring:

$$N_n = \frac{n}{g}\frac{\sigma}{\rho_l} \leqslant N_{n,2},$$

$$N_{n,2}^{3/325} = 0.71(1-\kappa)^{147/650}(1+1.455\kappa)^{93/650} \quad N_\sigma \geqslant 1. \tag{33}$$

(In both these inequalities, we have intentionally retained rather unwieldy exponents since reducing these inequalities to those for N_n would inevitably induce a noticeable error in relevant numerical coefficients.) It follows from inequality (32) at $\kappa \ll 1$ that N_n must exceed 11–12. Thus, for water at normal pressure and gravity, this requires n to be larger than approximately 150 cm^{-1}, whereas for other liquids, n must be even higher for lateral bubble coalescence to precede the two-phase flow crisis. On the contrary, inverted inequality (33) formally demands n to be smaller than a negligibly small quantity.

This shows that even in the case of $N_\sigma \leqslant 0.1$, the lateral bubble coalescence is not likely to generate extended vapour patches, nor cause the merging of neighbouring bubbles in general, prior to the isolated bubble regime being terminated by the two-phase flow crisis. If $N_\sigma \geqslant 1$, this coalescence seems altogether impossible. However, there exists a narrow intermediate region of parameter N_σ where lateral bubble coalescence can actually occur prior to the two-phase flow flooding-up crisis as wall temperature increases. Thus, we have to conclude that lateral growing bubble coalescence is usually irrelevant for the breakup of the isolated bubble boiling regime.

5. LONGITUDINAL BUBBLE COALESCENCE

Let us next consider the conditions under which the isolated bubble boiling regime comes to an end prior to the two-phase flow crisis occurring in the bulk and as a result of bubble coalescence in the direction normal to the wall. One should distinguish between merging couples of sequentially released bubbles from the same nucleation site near the wall and the coalescence of a chain of bubbles rising in the bulk. The former process leads to the establishment of a multiple bubble regime, whereas the latter one results in the formation of vapour columns.

5.1. *Coalescence near the wall*

A bubble growing at a nucleation site merges with its predecessor that has just detached if the velocity of the upper point on the growing bubble surface happens to be higher than the velocity of the bottom point of the preceding bubble. (The same idea was advantageously exploited in the theory of a gaseous bubble formation at submerged nozzles and plate orifices [30].) Presumably, the new bubble is sufficiently small for its growth to be inertially controlled. In this case, its top velocity can be expressed as [31]

$$\frac{dR}{dt} = \left[b\frac{\kappa}{1-\kappa}L\frac{\Delta T}{T_s}\right]^{1/2}. \tag{34}$$

Here, b is a numerical coefficient that equals $\pi/7$ for a sphere that expands when touching a plate, and equals 2/3 for a sphere expanding in an unbounded liquid. The same value of 2/3 has relevance to an expanding hemisphere whose base rests on the wall, if the formation of a viscous boundary layer in the liquid near the wall may be overlooked. Since the initial bubble shape must be approximately hemispherical [3, 4], we shall take $b = 2/3$.

At $N_\sigma \leqslant 0.1$, equation (5) yields an approximate solution $s = L_s\tau^2/5$. Hence, the departed bubble bottom velocity is equal to

$$\left(\frac{ds}{dt} - \frac{dR}{dt}\right)_d \approx \frac{L_s}{L_t}\left(\frac{2}{5}\tau_d - \frac{1}{2\sqrt{\tau_d}}\right) \approx \frac{3}{10}\frac{L_s}{L_t}\tau_d. \tag{35}$$

Using equations (4), (7) and equating the velocities in equations (34) and (35), we obtain after a manipulation, the wall overheat equation for longitudinal bubble coalescence

$$(CN_J)_{III} \approx 0.322\left(\frac{1+1.455\kappa}{1-\kappa}\right)^2\left(\frac{\kappa}{1-\kappa}\frac{L}{CN_{J,s}}\right)^3 \times \frac{1}{\chi^2 g^2} \quad N_\sigma \leqslant 0.1 \tag{36}$$

where $CN_{J,s}$ is expressed in terms of T_s in exactly the same way as CN_J is expressed through $\Delta T = T_w - T_s$. A significant feature of equation (36) consists in the fact that it does not involve n at all.

When comparing the critical Jakob number value in equation (35) with that specified in equation (24), we conclude that longitudinal bubble coalescence occurs near the wall at a smaller wall temperature than that of two-phase flow crisis, if

$$n^{3/10} \leqslant 1.24 \frac{(1-\kappa)^{99/40}}{(1+1.455\kappa)^{21/10}} g^{87/40} \left(\frac{\sigma}{\rho_l}\right)^{3/40} \times \chi^{3/2} \left(\frac{\kappa}{1-\kappa} \frac{L}{CN_{J,s}}\right)^{-3} \quad N_\sigma \leqslant 0.1. \quad (37)$$

In the case of $N_\sigma \geqslant 1$, s may be approximately expressed as a linear function of dimensionless time τ. Then we obtain, instead of equation (35),

$$\left(\frac{ds}{dt} - \frac{dR}{dt}\right)_d \approx \frac{L_s}{L_t}\left(\frac{1}{\sqrt{\tau_d}} - \frac{1}{2\sqrt{\tau_d}}\right) = \frac{L_s}{2L_t\sqrt{\tau_d}}. \quad (38)$$

Equating now the quantities in equation (34) and (38), we arrive at the critical wall overheat equation that replaces equation (36)

$$(CN_J)_{III} \approx 0.41 \frac{(1-\kappa)^{1/2}}{(1+1.455\kappa)^{31/32}} \frac{g^{11/32}}{\chi^{1/8}} \left(\frac{\sigma}{\rho_l}\right)^{15/32} \times \left(\frac{\kappa}{1-\kappa} \frac{L}{CN_{J,s}}\right)^{-3/4} \quad N_\sigma \geqslant 1. \quad (39)$$

In this case of appreciable N_σ, the condition of longitudinal coalescence near the wall that precedes the two-phase flow crisis takes the form:

$$n^{6/25} \leqslant 1.26 \frac{(1+1.455\kappa)^{651/800}}{(1-\kappa)^{3/25}} \times \frac{1}{g^{183/192}(\sigma/\rho_l)^{267/192}\chi^{75/48}} \left(\frac{\kappa}{1-\kappa} \frac{L}{CN_{J,s}}\right)^{3/4} \quad N_\sigma \geqslant 1. \quad (40)$$

This inequality is also somewhat "inverted" as compared with inequality (37).

The critical heat flux densities that correspond to the beginning of longitudinal bubble coalescence at the wall can be expressed with the help of equations (15) and (16) when using equations (36) and (39), respectively. However, these equations are not of much use since as a result of coalescence, the onset of the multiple bubble boiling regime does not lead to essential changes in heat transfer characteristics as compared with those for the isolated bubble regime. Both inequalities (37) and (40) require nucleation site population density to be sufficiently small for longitudinal bubble coalescence at the wall to occur at a smaller wall temperature than the two-phase flow crisis in the bulk does. This is quite understandable since an increase in this density lowers the critical wall overheat for the two-phase flow crisis in conformity with equations (24) and (25), whereas the critical overheat for longitudinal coalescence does not depend on nucleation site density at all, in accordance with equations (36) and (39). A simple evaluation shows that these requirements can be satisfied at values of the involved parameters that are encountered in practice.

5.2. *Coalescence in the bulk*

A chain of bubbles rising in succession from the same nucleation site cannot exist, and instead it must form a continuous vapour bubble column if, for time t_d, any bubble covers a distance that exceeds the bubble diameter. (This requirement was often used in precisely the same context in many papers on nucleate boiling and in particular in [2].) Thus, the general condition for the generation of vapour columns can be formulated as follows:

$$2R_d/t_d = U_b \quad (41)$$

bubble velocity being assumed dependent on the bubble volume concentration in accordance with equation (20).

For the sake of simplicity, we shall confine ourselves to treating the case of $\kappa \ll 1$. In this case, an equation to solve for ϕ follows from equations (19)–(21). It reads

$$\phi(1-\phi) = \frac{q}{\rho_v[c_l(T_s - T_\infty) + L]U_b^\circ} \approx \frac{1}{K_u g^{1/4}(\sigma/\rho_l)^{1/4}} \frac{q}{\rho_v[c_l(T_s - T_\infty) + L]}. \quad (42)$$

If $N_\sigma \leqslant 0.1$, we have to make use of equation (15) for q. After some calculation, we arrive at the following equation:

$$1 - \phi \approx \frac{1}{2}\left\{1 + \left[1 - \left(\frac{CN_J}{(CN_J)_I}\right)^{10/3}\right]^{1/2}\right\} \quad N_\sigma \leqslant 0.1 \quad (43)$$

where $(CN_J)_I$ stands for the critical Jakob number identified in equation (24). Now using equation (41) with R_d and t_d from equation (8) and with $1-\phi$ from equation (43), we get an algebraic equation that determines the critical wall overheat at which vapour columns start to originate,

$$\frac{x^{2/3}}{\{1 + [1 - x^{10/3}]^{1/2}\}} \approx 0.82 N_n^{1/5}$$

$$x \equiv \frac{(CN_J)_{IV}}{(CN_J)_I} \quad N_\sigma \leqslant 0.1 \quad (44)$$

with N_n being defined in equation (32). This equation has an approximate solution which ought to be rather good at sufficiently small x (or sufficiently small N_n)

$$x \approx 2.1 N_n^{3/10}. \quad (45)$$

If $x = x(N_n) \leqslant 1$, then longitudinal coalescence of bubble rising in the bulk indeed starts at a smaller wall temperature than the two-phase flow flooding-up crisis. This happens at N_n smaller than approximately unity. In normal gravity, values of N_n commonly fall within the range $(0.01, 1)$. Therefore, longitudinal bubble coalescence with formation of vapour columns practically always precedes the two-phase flow crisis at normal gravity conditions. However, this is not

necessarily so in reduced gravity because $N_n \sim g^{-1}$ increases as g decreases, and can well be much larger than unity. Of course, this conclusion is subject to the condition that g is not too low to render N_σ comparable to unity.

The critical heat flux that corresponds to the onset of longitudinal coalescence can be expressed with the aid of equations (15) and (23) and the above definition of x in the following form:

$$q_{IV} \approx Q\left(g\frac{\sigma}{\rho_l}\right)^{1/4} \rho_v[c_l(T_s - T_\infty) + L]$$

$$Q = \frac{K_u}{4} x^{10/3}(N_n) \quad N_\sigma \leqslant 0.1. \tag{46}$$

It is easy to conclude that coefficient Q in this equation decreases by an order of magnitude as N_n decreases from unity to 0.01.

A similar calculation for the case of $N_\sigma \geqslant 1$ can also be performed on the basis of equations (41) and (42) when using equations (11) and (16) instead of equations (8) and (15). As a result, we obtain a new transcendental equation for x,

$$x^{1/6}\{1 + [1 - x^{25/6}]^{1/2}\} \approx 0.85 N_n^{1/25}$$

$$x = \frac{(CN_J)_{IV}}{(CN_J)_I} \quad N_\sigma \geqslant 1. \tag{47}$$

which has the approximate solution which substitutes for solution (45)

$$x \approx 6.06 \times 10^{-3} N_n^{6/25} \quad N_\sigma \geqslant 1. \tag{48}$$

This approximate solution practically coincides with the exact solution to equation (47).

The corresponding critical heat flux can be formulated in the same form as equation (46) but for coefficient Q being differently defined,

$$q_{IV} \approx Q\left(g\frac{\sigma}{\rho_l}\right)^{1/4} \rho_v[c_l(T_s - T_\infty) + L]$$

$$Q = \frac{K_u}{4} x^{25/6}(N_n) \quad N_\sigma \geqslant 1. \tag{49}$$

At $N_\sigma \geqslant 1$, coefficient Q is extremely smaller than its value of $K_u/4$ which is specific to the two-phase flow crisis. This means that bubbles begin to coalesce and to form vapour columns at much smaller wall temperatures than those at which the two-phase flow crisis normally occurs in the bulk, provided that the surface tension force plays a noticeable role in promoting bubble detachment (parameter N_σ is larger than unity).

6. DISCUSSION

On the whole, we have succeeded in (1) deriving informative formulae pertaining to the hydrodynamic and heat transfer characteristics of the isolated bubble regime of pool nucleate boiling, and (2) outlining the conditions under which this regime terminates as well as disclosing the possible physical causes and effects of its termination. These formulae do not involve adjustable parameters and new arbitrary constants except for those describing the rate of thermally controlled bubble growth and bubble rise velocity. However, all the results and findings of this work are restricted to an idealized boiling system that is geometrically simple and to the case of thermally controlled bubble growth. However, final numerical results can at present be obtained only for walls with a set of artificial nucleation cavities (that is, at known constant n). In order to treat more general cases of walls with natural activated nucleation sites, we need n as a function of wall overheat. The determination of such a function certainly goes beyond the intended scope of this paper.

It has been shown that not only bubble detachment size and frequency, but also the heat flux density specific to both the isolated bubble boiling regime and the conditions of this regime breakup are strongly dependent on the balance of the major forces that bring about bubble detachment. Two extreme cases can be singled out: one in which the buoyancy force dominates the bubble detachment process, and one in which the surface tension force prevails. As the role played by the surface tension force in this process grows, bubbles become progressively smaller (their detachment size decreases as $N_\sigma^{-5/16}$), and bubble detachment frequency increases proportionally to $N_\sigma^{5/8}$. Hence, the total volume of vapour produced at a single nucleation site reduces as $N_\sigma^{-5/16}$, all other things being equal. This also results in a corresponding decrease in the heat flux removed from a heated surface which causes, in turn, a stronger heat flux dependence on wall temperature.

If bubble detachment is stipulated by buoyancy, as is the case at $N_\sigma \leqslant 0.1$, the isolated bubble boiling regime normally breaks up due to the longitudinal coalescence of bubbles rising in the bulk which leads to the generation of vapour columns. In moderately reduced gravity, the two-phase flow flooding-up crisis can precede coalescence and can thereby cause this regime termination. This flooding-up crisis results because the swarm of rising vapour bubbles prevents liquid from coming to the heated wall to be evaporated and so inhibits compensation for vapour outflow with the bubbles.

If bubble detachment is mostly caused by the surface tension force, as it happens at $N_\sigma \geqslant 1$, the isolated bubble boiling regime always comes to an end as a result of longitudinal bubble coalescence in the bulk, so that the two-phase flow flooding-up crisis does not take place at all. This coalescence occurs at much smaller wall overheats than those specific to coalescence under the buoyancy-driven bubble departure conditions.

Irrespective of whether buoyancy or surface tension prevails in bubble detachment, longitudinal coalescence of bubbles in the immediate vicinity of the wall

can take place under certain conditions. This type of coalescence results in the establishment of the multiple bubble regime of pool nucleate boiling. However, boiling heat transfer characteristics do not drastically change simply because the isolated bubble regime has been replaced by the multiple bubble regime. The lateral coalescence of bubbles evolving at neighbouring sites does not noticeably participate in the transition from the isolated bubble regime to the multiple bubble regime, and on the whole appears to be insignificant.

Dependence of the critical heat fluxes and wall overheats on various parameters is very complicated. This is due to the fact that most of the parameters simultaneously affect quite different phenomena that are significant for nucleate boiling as a whole. It is rather difficult to formulate unequivocal inferences as concerns the influence of any parameter on boiling characteristics. Under different conditions, the projected influence may turnout to be quite different as well.

Consider, by the way of example, the effect caused by gravity. In the first place, gravity acceleration affects the length and time scales of bubble evolution on the wall and thereby conditions bubble detachment characteristics in its own right. Secondly, any change in g leads to a corresponding change in N_σ, and this results in a modification of the relative parts taken by buoyancy and surface tension in ensuring bubble detachment, and hence causes an additional effect on the bubble detachment size and frequency. Besides this, gravity acceleration affects bubble rise velocity, and this greatly influences the conditions for the onset of both the two-phase flow crisis and the longitudinal bubble coalescence in the bulk. The interplay of these manifold effects produces a very complicated gravity dependence for all the critical heat fluxes and wall overheats, and this can be observed in practice.

For instance, at $N_\sigma \leqslant 1$, the ratio of the heat flux in an arbitrary gravity to that in normal Earth gravity can be formulated from equation (46) as follows:

$$\frac{q_{\mathrm{IV}}}{q_{\mathrm{IV,e}}} = \left(\frac{g}{g_{\mathrm{e}}}\right)^{1/4} \frac{x^{10/3}}{x_{\mathrm{e}}^{10/3}}$$

$$x = x(N_{\mathrm{n}}) \quad x_{\mathrm{e}} = x(N_{\mathrm{n,e}}) \quad N_\sigma \leqslant 0.1 \qquad (50)$$

x being understood as the root of equation (44).

If $N_{\mathrm{n,e}}$ is close to unity, then a decrease of g causes N_{n} to increase. This increase in N_{n} causes the two-phase flow crisis to replace longitudinal bubble coalescence, and this is the physical mechanism that is responsible for the isolated bubble boiling regime termination. In this case, equation (50) holds true as well, with both x and x_{e} being substituted by unity. Thus, we reproduce the well-known proportionality of the critical heat flux to $g^{1/4}$ [32].

If $N_{\mathrm{n,e}}$ is small enough, a relatively moderate decrease in g does not alter the bubble coalescence mechanism for the isolated bubble regime breakup. However, the ensuing increase in N_{n} produces a corresponding increase in x, which in its turn, makes ratio (50) decrease slower than required by the aforementioned proportionality of the critical heat flux to $g^{1/4}$. In the extremal case of exceedingly low N_{n}, x may be expressed as it is in equation (45). In this case, we are able to conclude from equation (50) and from the definition of N_{n} in equation (32) that ratio (50) is proportional to $g^{-3/4}$. The same proportionality is valid for the case of $N_\sigma \geqslant 1$ when it immediately results from equations (48) and (49) and from the definition of N_{n}. This means that the critical heat flux has to grow, and to grow sufficiently fast, as g diminishes.

In the intermediate range of N_{n}, the critical heat flux may increase or decrease with g, depending on values of other relevant parameters. Deviations from the law $q_{\mathrm{IV}}/q_{\mathrm{IV,e}} = N_g^{1/4}$ that had been observed about three decades ago were summarized and discussed in ref. [32]. More recent observations of the same kind are listed in ref. [33] where an increase in the boiling heat transfer that accompanies a decrease in g is also reported. On the whole, the above conclusions help us to understand these experimental observations.

In the course of our analysis, we have reproduced a number of semi-empirical formulae and purely empirical correlations that were broadly used to describe boiling hydrodynamics and heat transfer. It is quite evident that our equations are supported by experimental evidence to not a lesser extent than the previously used semi-empirical and empirical formulae. However, our equations possess an advantage over the usually employed formulae: they do not require that numerical coefficients and numerical exponents be determined from experiments. Moreover, they help us to explain why such coefficients and exponents commonly vary within rather wide intervals and are not reproducible from experiment to experiment.

A representative example is given by the critical heat flux specified in equation (23). The theoretical numerical coefficient in this equation equals 0.295 at $K_{\mathrm{u}} = 1.18$ [22] or 0.3825 at $K_{\mathrm{u}} = 1.53$ [23], and these values are somewhat higher than the average empirical coefficients of 0.13–0.18 [1]. However, equations (46) and (49) show that this coefficient diminishes as the two-phase flow crisis gives way to bubble coalescence in the bulk when it serves as a major mechanism that favours the isolated bubble regime termination. If $N_\sigma \leqslant 0.1$, such a coefficient can be several times as small as its value that is associated with the two-phase flow crisis. If $N_\sigma \geqslant 1$, this coefficient decrease can amount to a few order of magnitude.

It should be remembered, of course, that the isolated bubble boiling crisis under discussion must be distinguished from the usually studied CHF (or burnout) crisis. Nevertheless, the two-phase flow crisis certainly results in the generation of excessive vapour volumes near the wall. Therefore, it is hardly unlikely that the difference between the critical heat flux determined in this paper and the usually treated CHF is appreciably great. Similarly, longitudinal bubble coal-

escence in the bulk leads to the formation of vapour columns which are certainly bound to be hydrodynamically unstable. The merging of such columns due to instability must result in the formation of extended vapour masses linked to the heated wall by short vapour jets. Again, the difference between the critical heat flux under discussion and the usually studied CHF ought not to be great as compared with any one of the critical heat densities under question. At any rate, this is true in the limiting case of $N_\sigma \leqslant 0.1$.

The case of $N_\sigma \geqslant 1$ may present an exception since equation (49) gives exceedingly low values for the critical heat flux density that corresponds to the formation of vapour columns. This means that the mentioned critical heat flux difference may well be comparable to any of the critical heat fluxes under discussion. In these circumstances, a more sophisticated model of the burnout crisis is needed. Presumably, such a model must be developed along the lines indicated earlier in ref. [34].

In conclusion, we wish to once again emphasize the urgent necessity to find out a representative expression for the site population density as a function of wall overheat in order to finally close some of the equations listed in this paper. Since such a function must also depend on poorly determinable characteristics of the superheated wall surface, its determination represents a formidable task of the theory of nucleation and incipient boiling. For this reason, it is likely that appropriate semi-empirical functions of wall overheat should be used for this purpose.

Acknowledgement—This paper was written while Prof. Yu. Buyevich held a National Research Council Research Associateship at the NASA Ames Research Center.

REFERENCES

1. W. M. Rohsenow, Boiling. In *Handbook of Heat Transfer*, pp. 13.1–13.75. McGraw-Hill, New York (1973).
2. N. Zuber, Nucleate boiling. The region of isolated bubbles and the similarity with natural convection, *Int. J. Heat Mass Transfer* **6**, 53–78 (1963).
3. Yu. A. Buyevich and B. W. Webbon, Modeling of vapor bubble growth under nucleate boiling conditions in reduced gravity, paper 95-WA/HT-42, *ASME Int. Mech. Engng Congr. and Exposition*, San Francisco, California (1995).
4. Yu. A. Buyevich and B. W. Webbon, Dynamics of vapour bubbles in nucleate boiling, *Int. J. Heat Mass Transfer* **39**, 2409–2426 (1996).
5. T. Diesselhorst, U. Grigull and E. Hahne, Hydrodynamic and surface effects on the peak heat flux in pool boiling. In *Heat Transfer in Boiling*, pp. 99–135. Hemisphere, Washington, D.C. (1977).
6. Y. Katto, Critical Heat Flux, *Advances in Heat Transfer*, Vol. 17, pp. 1–64. Academic Press, New York (1985).
7. W. M. Rohsenow and P. Griffith, Correlation of maximum heat transfer data for boiling of saturated liquids, *Chem. Engng Progr. Symp. Ser.* **52**, 47–54 (1956).
8. R. Cole and W. M. Rohsenow, Correlation of bubble departure diameters for boiling of saturated liquids, *Chem. Engng Progr. Symp. Ser.* **65**(92), 211–213 (1969).
9. S. S. Kutateladze, A hydrodynamic model of the critical heat transfer in boiling liquids with free convection, *Zh. Tekhn. Fiz.* **20**, 1389–1395 (1950).
10. N. Zuber, On the stability of boiling heat transfer, *Trans. ASME* **80**, 711–720 (1958).
11. Y. P. Chang and N. M. Snyder, Heat transfer in saturated boiling, *Chem. Engng Progr. Symp. Ser.* **56**, 25–38 (1960).
12. S. S. Kutateladze, *Fundamentals of Heat Transfer*. Academic Press, New York (1963).
13. Y. Haramura and Y. Katto, A new hydrodynamic model of critical heat flux, applicable widely to both pool and forced convection boiling on submerged bodies in saturated liquids, *Int. J. Heat Mass Transfer* **26**, 389–399 (1983).
14. A. K. Rajvanshi, J. S. Saini and R. Prakash, Investigation of macrolayer thickness in nucleate pool boiling at high heat flux, *Int. J. Heat Mass Transfer* **35**, 343–350 (1992).
15. T. Kumada and H. Sakashita, Pool boiling heat transfer—II. Thickness of liquid macrolayer formed beneath vapor masses, *Int. J. Heat Mass Transfer* **38**, 979–987 (1995).
16. Y. Katto, A prediction model of subcooled boiling CHF for pressure in the range 0.1–20.0 MPa, *Int. J. Heat Mass Transfer* **35**, 1115–1123 (1992).
17. G. P. Celata, M. Cumo, A. Mariani and G. Zummo, The prediction of the critical heat flux in water-subcooled flow boiling, *Int. J. Heat Mass Transfer* **38**, 1111–1119 (1995).
18. A. Serizawa, Theoretical prediction of maximum heat flux in power transients, *Int. J. Heat Mass Transfer* **26**, 921–932 (1983).
19. O. Pasamehmetoglu, R. A. Nelson and F. S. Gunnerson, Critical heat flux modeling in pool boiling for steady-state and power transients, *Trans. ASME, J. Heat Transfer* **112**, 1048–1057 (1990).
20. W. Körner and G. Photiadis, Pool boiling heat transfer and bubble growth on surfaces with artificial cavities for bubble generation. In *Heat Transfer in Boiling*, pp. 77–84. Hemisphere, Washington, D.C. (1977).
21. R. Cole, A photographic study of pool boiling in the region of the critical heat flux, *A.I.Ch.E.Jl* **6**, 533–537 (1960).
22. P. W. McFadden and P. Grassman, The relation between bubble frequency and diameter during nucleate pool boiling, *Int. J. Heat Mass Transfer* **5**, 169–176 (1962).
23. H. J. Ivey, Relationships between bubble frequency, departure diameter and rise velocity in nucleate boiling, *Int. J. Heat Mass Transfer* **10**, 1023–1040 (1967).
24. W. Bergez, Nucleate boiling on a thin heating plate: heat transfer and bubbling activity of nucleation sites, *Int. J. Heat Mass Transfer* **38**, 1799–1811 (1995).
25. G. B. Wallis, *One-Dimensional Two-Phase Flow*. McGraw-Hill, New York (1969).
26. Yu. A. Buyevich, Collective effects in a concentrated system of large bubbles, *Inzh.-Fiz. Zh.* **46**, 1057–1066 (1981).
27. F. N. Peebles and H. J. Garber, Studies on the motion of gas bubbles in liquids, *Chem. Engng Progr.* **49**, 88–95 (1953).
28. T. Harmathy, Velocity of large drops and bubbles in media of infinite or restricted extent, *A.I.Ch.E.Jl* **6**, 281–288 (1960).
29. J. M. Ziman, *Models of Disorder. The Theoretical Physics of Homogeneously Disordered Systems*. Cambridge University Press, Cambridge (1979).
30. J. K. Walters and J. F. Davidson, The initial motion of a gas bubble formed in an inviscid liquid. Part 2. The three-dimensional bubble and the toroidal bubble, *J. Fluid Mech.* **17**, 321–336 (1963).
31. B. B. Mikic, W. M. Rohsenow and P. Griffith, On bubble growth rates, *Int. J. Heat Mass Transfer* **13**, 657–666 (1970).

32. R. Siegel, Effects of reduced gravity on heat transfer, *Advances in Heat Transfer*, Vol. 4, pp. 143–228. Academic Press, New York (1967).
33. J. Straub, M. Zell and B. Vogel, Pool boiling in a reduced gravity field. *Heat Transfer* 1990, *Proc. Ninth Int. Heat Transfer Conf.*, Jerusalem, Vol. 1, pp. 91–112. Hemisphere, New York (1990).
34. V. K. Dhir, Nucleate and transition boiling heat transfer under pool and external flow conditions, *Int. J. Heat and Fluid Flow* **12**, 290–314 (1991).